Journal of Biomedical Optics

SPIEDigitalLibrary.org/jbo

Time-resolved fluorescence spectroscopy investigation of the effect of 4-hydroxynonenal on endogenous NAD(P)H in living cardiac myocytes

Alzbeta Chorvatova
Swida Aneba
Anton Mateasik
Dusan Chorvat, Jr.
Blandine Comte

SPIE

Time-resolved fluorescence spectroscopy investigation of the effect of 4-hydroxynonenal on endogenous NAD(P)H in living cardiac myocytes

Alzbeta Chorvatova,[a,b] Swida Aneba,[b] Anton Mateasik,[a] Dusan Chorvat Jr.,[a] and Blandine Comte[b,c]
[a]International Laser Center, Department of Biophotonics, Ilkovicova 3, 84104 Bratislava, Slovakia
[b]University of Montreal, Research Centre, Centre Hospitalier Universitaire Sainte-Justine, H3T 1C5 Montreal, Quebec, Canada
[c]Clermont Université, Université d'Auvergne, Unité de Nutrition Humaine, BP 10448, INRA, UMR 1019, UNH, CRNH Auvergne, F-63000 Clermont-Ferrand, France

Abstract. Lipid peroxidation is a major biochemical consequence of the oxidative deterioration of polyunsaturated lipids in cell membranes and causes damage to membrane integrity and loss of protein function. 4-hydroxy-2-nonenal (HNE), one of the most reactive products of n-6 polyunsaturated fatty acid peroxidation of membrane phospholipids, has been shown to be capable of affecting both nicotinamide adenine dinucleotide (phosphate) reduced [NAD(P)H] as well as NADH production. However, the understanding of its effects in living cardiac cells is still lacking. Our goal was to therefore investigate HNE effects on NAD(P)H noninvasively in living cardiomyocytes. Spectrally resolved lifetime detection of endogenous fluorescence, an innovative noninvasive technique, was employed. Individual fluorescence components were resolved by spectral linear unmixing approach. Gathered results revealed that HNE reduced the amplitude of both resolved NAD(P)H components in a concentration-dependent manner. In addition, HNE increased flavoprotein fluorescence and responsiveness of the NAD(P)H component ratio to glutathione reductase (GR) inhibitor. HNE also increased the percentage of oxidized nucleotides and decreased maximal NADH production. Presented data indicate that HNE provoked an important cell oxidation by acting on NAD(P)H regulating systems in cardiomyocytes. Understanding the precise role of oxidative processes and their products in living cells is crucial for finding new noninvasive tools for biomedical diagnostics of pathophysiological states. [DOI: 10.1117/1.JBO.18.6.067009]

Keywords: endogenous nicotinamide adenine dinucleotide (phosphate) reduced fluorescence; time-resolved fluorescence spectrometry; oxidative stress; 4-hydroxynonenal; cardiomyocyte energy metabolism.

Paper 130107R received Feb. 28, 2013; revised manuscript received May 23, 2013; accepted for publication May 29, 2013; published online Jun. 26, 2013.

1 Introduction

4-hydroxy-2-nonenal (HNE) is the primary α,β-unsaturated hydroxyalkenal formed in cells by lipid peroxidation (LPO) process.[1] It is generated in the peroxidation of lipids containing polyunsaturated omega-6 acyl groups, such as arachidonic or linoleic acids, and of the corresponding fatty acids. HNE has three reactive groups: an aldehyde, a double bond at carbon 2, and a hydroxy group at carbon 4. It is found throughout animal tissues and in higher quantities during oxidative stress due to the increase in lipid peroxidation chain reaction, elevated in stress events. The oxidative degradation of lipids affects mostly polyunsaturated fatty acids, because they contain multiple double bonds in between which lies methylene–CH_2– groups that possess especially reactive hydrogens. Living organisms have generated different molecules that speed up termination by catching free radicals and therefore protect cell membranes.[2] Such antioxidants include alpha-tocopherol, also known as vitamine E, as well as enzymes such as superoxide dismutase, catalase, and glutathione peroxidases. HNE plays a key role in the cell signaling transduction in a variety of pathways from cell cycle events to cellular adhesion.[3] Constitutive levels of HNE are needed for normal cell functions—their lowering in cells promotes proliferative machinery, while their increase stimulates apoptotic signaling.[4,5]

In cardiac myocytes, HNE has been shown to be capable of affecting nicotinamide adenine dinucleotide (phosphate) reduced [NAD(P)H] production by inactivating mitochondrial $NADP^+$-isocitrate dehydrogenase activity, an important enzyme that controls redox and energy status.[6–8] In addition, in isolated cardiac mitochondria, it has been reported that HNE inhibited α-ketoglutarate dehydrogenase and reduced the production of NADH.[9] However, the exact effects of HNE on NAD(P)H fluorescence in cardiac cells are still poorly understood. We have previously showed the sensitivity of NAD(P)H fluorescence to oxidative stress induced by stressors such as hydrogen peroxide (H_2O_2) or HNE in living left ventricular (LV) myocytes (see Supplement in Ref. 10 for details). Here, our goal was to evaluate in further detail the effect of HNE on the NAD(P)H content in order to better understand mechanisms underlying HNE action in these cells.

We have chosen time-resolved fluorescence spectroscopy of intrinsic NAD(P)H (Ref. 11) to test the effect of HNE in living myocytes. We have previously demonstrated that both the NADH, as well as the spectroscopically undistinguishable NADPH can be measured directly and noninvasively in rat cardiac myocytes by this novel method.[12–14] In rat liver, the total

Address all correspondence to: Alzbeta Chorvatova, International Laser Center, Department of Biophotonics, Ilkovicova 3, 84104 Bratislava, Slovakia. Tel: 0421 2 65421575; Fax: +4212654 23 244; E-mail: alzbeta.chorvatova@ilc.sk

0091-3286/2013/$25.00

amount of NAD^+ and NADH is approximately 1 μmole per gram of wet weight, about 10 times the concentration of $NADP^+$ and NADPH in the same cells.[15] The cellular $NADPH/NADP^+$ ratio is normally about 200, around 200 times lower than the one of $NADH/NAD^+$, which ranges from 1 to 0.1 between mitochondria and cytosol, respectively.[16,17] The $NADPH/NADP^+$ ratio is kept very high because NADPH is needed to drive redox reactions as a strong reducing agent and regulator of the redox homeostasis in mammalian cells. However, this proportion is prone to change in pathological situations, such as oxidative stress. For these reasons, we have chosen evaluation of endogenous NAD(P)H fluorescence to examine the effect of HNE. To precisely comprehend modifications in the oxidative redox state from the recorded data, we have chosen a new analytical approach based on evaluation of the individual components in the time-resolved fluorescence spectroscopy measurements using principal component analysis (PCA) and resolve them by a linear unmixing approach.[14] In this way, "free" and "bound" NAD(P)H components can be precisely separated and the effects of HNE studied on the resolved individual components. As the ratio of free/bound component amplitude corresponds to the change in $NAD(P)H/NAD(P)^+$ reduction/oxidation pair,[13,14,18,19] this approach thus allows an original monitoring of HNE actions.

2 Material and Methods

2.1 *Ethics Approval*

All procedures were performed in accordance with the National Institute of Health and the Canadian Council on Animal Care (CCAC) guidelines for the care and use of laboratory animals, after evaluation by the local Comité Institutionnel des Bonnes Pratiques sur les Animaux en Recherche, accredited by the CCAC.

2.2 *Cell Isolation*

Cardiac myocytes were isolated from LV of Sprague-Dawley rats (13- to 14-week-old females, Charles River, Canada) sacrificed humanely by decapitation after retrograde perfusion of the heart with proteolytic enzymes, as previously reported.[20,21] Myocytes were maintained in storage solution at 4°C until used. Only cardiac myocytes showing clearly defined striations and edges were studied.

2.3 *NAD(P)H and Flavin Fluorescence*

Endogenous fluorescence of NAD(P)H and flavins was recorded using spectrally resolved time-correlated single photon counting, as previously described.[14,22] In these experiments, a 375-nm, or a 435-nm, picosecond laser diode (BDL-375, BDL-435, Becker&Hickl, Boston Electronics, USA) was used as an excitation source with ~1 mW output power. The laser beam was reflected to the sample through the epifluorescence path of the Axiovert 200M (Zeiss, Canada) inverted microscope. The emitted fluorescence was separated from laser excitation either by 395-nm dichroic and 397-nm long-pass filter (for excitation at 375 nm) or by 460-nm dichroic filter and 470-nm long-pass filter (for excitation at 438 nm) and detected by 16-channel photomultiplier array (PML-16, Becker&Hickl, Boston Electronics) attached to an imaging spectrograph (Solar 100, Proscan, Germany). Data were always evaluated from the first scan of each cell (measured for 30 s) to avoid artifacts induced by photobleaching.

2.4 *Solutions and Drugs*

The storage solution contained (in mM) NaCl, 130.0; KCl, 5.4; $MgCl_2 \cdot 6H_2O$, 1.4; NaH_2PO_4, 0.4; creatine, 10.0; taurine, 20.0; glucose, 10.0; and 4-(2-hydroxyethyl)-1-piperazineethanesulfonic acid (HEPES), 10.0; titrated to pH 7.30 with NaOH. The basic external solution contained (in mM): NaCl, 140.0; KCl, 5.4; $CaCl_2$, 2.0; $MgCl_2$, 1.0; glucose, 10.0; HEPES, 10.0, adjusted to pH 7.35 with NaOH. The intracellular media-mimicking solution contained (in mM) KCl, 140; NaCl, 10; glucose, 10; HEPES, 10, adjusted to pH 7.25 with NaOH. NADPH was added to the intracellular solution in concentrations ranging from 1 to 20 μM. NADPH was also produced from NADP-isocitrate dehydrogenase (ICDH) (3.9 U/mL) by reaction of isocitrate (89 mM) and NADP (0.5 mM) with or without glutathione [glutathione disulfide (GSSG), 50 nM] and GR (0.5 or 1 U/mL). Cells were treated (in basic external solution for 30 min at 35°C) with 1,3-bis(2-chloroethyl)-1-nitroso-urea (BCNU, 100 μM) and/or HNE (10, 25, 50, or 100 μM), or H_2O_2 (1 μM), and recorded at room temperature. Rotenone (1 μM) with cyanide (4 mM) and/or 9,10-dinitrophenol (DNP, 50 μM) were applied for 5 to 10 min before recording; 3-β-hydroxybutyrate (BHB, 3 mM) was prepared freshly, while acetoacetate (AcAc, 150 μM to obtain a BHB/AcAc ratio of 20:1, and 1.5 mM to obtain a BHB/AcAc ratio of 2:1) was added from 250 mM stock solution. All chemicals were from Sigma-Aldrich (Canada), except for cyanide, which was from Fisher (Canada).

2.5 *Data Analysis*

The data are reported as means ± standard error error of the means. Data were collected from at least three different animals per experimental group and compared by one-way analysis of variance; $p < 0.05$ was considered statistically significant. Data were analyzed using SPCImage software (Becker&Hickl, Boston Electronics), Origin 7.0 (OriginLab, USA), laser scanning microscope Image Browser (Zeiss), and custom-written procedures for data correction and analysis written in C++. In our experiments, we typically collected a photon-counting histogram of spectrally resolved autofluorescence decay $P(\lambda_j, t_k)$. The histogram was measured simultaneously on 16 spectral channels (18-nm wide) denoted as λ_j and on 1024 temporal channels denoted as t_k, spaced equidistantly by 24.4 ps. Individual components of NAD(P)H fluorescence were determined by PCA, applying the linear unmixing approach to separate individual components in the recorded data, as previously reported.[13,14] Amplitudes of the resolved NAD(P)H fluorescence components were calculated by unmixing. The sum of amplitudes of all resolved components equals the total photon count in the measured experimental condition. Fluorescence lifetime was estimated using a monoexponential fitting procedure at the maximum intensity spectral channel (450 nm) for each decay component independently, with the assumption that the fluorescence decay is independent of emission wavelength. Intensity was calculated as [(component amplitude)× (fluorescence lifetime)] for each component. Relative spectral contribution was calculated as an integral intensity, where the component amplitude was multiplied by the unitary reference spectrum reported in Ref. 13. This spectrum is composed

from the one for NADH in organic solvents (represented by water) with maximum at 460 nm, for NADH in inorganic solvent (represented by glycerol) with maximum at 440 nm, and for flavin adenine dinucleotide (FAD) in water with maximum at 520 nm.

3 Results

3.1 *NADPH Fluorescence Recording In Vitro*

Fluorescence spectra and fluorescence lifetimes [Fig. 1(a)] of NADPH were studied *in vitro* in the intracellular media-mimicking solution (pH 7.25), as previously reported.[12] Steady-state emission spectra measured simultaneously at 16 acquisition channels were determined as the total photon counts on each spectral channel. Concentrations ranging from 1 to 20 μM of NADPH in intracellular media-mimicking solutions were used to test the dose-dependence of the NADPH fluorescence spectral intensity and fluorescence decays *in vitro*. As expected, the spectral intensity was linearly dependent on the NADPH concentration, as illustrated by the maximum emission wavelength of 450 nm [Fig. 1(a) right]; at the same time, we found no modification in the fluorescence decays [Fig. 1(a) middle]. Normalized spectra for NADPH concentrations from 1 to 20 μM overlaid perfectly (data not shown), confirming the same molecular origin. This result is in agreement with the effects induced by elevated NADH concentrations in aqueous solutions.[12,23]

To test the sensitivity to molecular environment, we have recorded NADPH fluorescence (10 μM) in solutions with different viscosity, achieved by the addition of glycerol (0, 25, 50, 75, and 100%) versus H_2O [Fig. 1(b)]. The total photon counts, measured at the emission maximum ($\lambda_{em} = 450$ nm), revealed exponential rise of the peak of NADPH fluorescence intensity with glycerol [Fig. 1(b) right]. We also noted a slight 10 nm blue spectral shift when NADPH fluorescence was recorded in a more viscous environment (data not shown). This result was due to the prolongation of the fluorescence lifetimes in a highly viscous environment [Fig. 1(b) middle] and is in agreement with

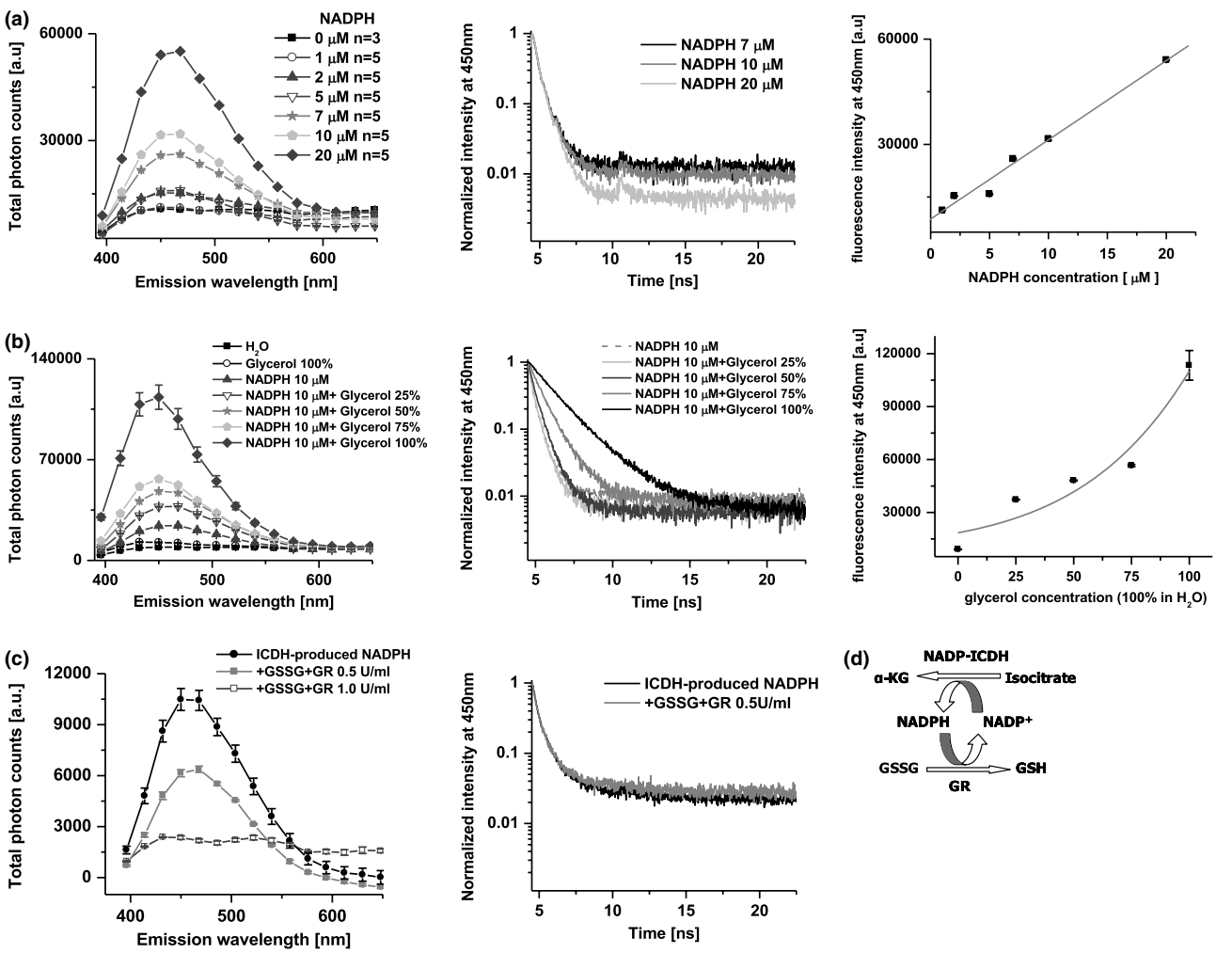

Fig. 1 NADPH fluorescence *in vitro*. (a) Concentration dependence of NADPH fluorescence in the intracellular media-mimicking solution (pH 7.25), excitation 375 nm. Background-corrected emission spectra (left), normalized fluorescence decays at 450 nm (middle), and the total photon counts at 450 nm (right) as a function of the NADPH concentration. (b) Viscosity dependence of NADPH (10 μM) fluorescence in intracellular solution. Background-corrected emission spectra (left), normalized fluorescence decays at 450 nm (middle), and the total photon counts at 450 nm (right) as a function of the glycerol concentration versus water. (c) $NADP^+$-ICDH produced NADPH fluorescence *in vitro* in the absence or presence of GR (0.5 or 1.0 U/ml) in intracellular solution. Blank-corrected emission spectra (left), normalized fluorescence decays at 450 nm (right). (d) Schematic representation of the induced reaction.

previous findings,[24] showing that the sensitivity of NADPH fluorescence intensity to changes in its microenvironment can be related to changes in the molecular mobility and/or modification in the conformation of NADPH molecules in more viscous milieu.

NADP-ICDH has been shown to play an important role in increasing NADPH pool in heart mitochondria, especially during oxidative stress.[25,26] NADPH is a cofactor that is essential for glutathione system, one of the defense mechanisms against oxidative stress. It is used by GR to convert GSSG to reduced glutathione (GSH), which is needed to detoxify H_2O_2 and change it into water.[27] GR is a flavoprotein, with functions to regenerate antioxidant capacity, converting from GSSG to the sulfhydryl form GSH. As the most important nonprotein thiol source, GSH plays a key role in the maintenance of cellular redox status and antioxidant defense. We have tested the capability of the experimental setup to monitor the NADPH produced by $NADP^+$-ICDH *in vitro* and the efficiency of GR to reverse this effect according to the schematic representation in Fig. 1(d). Our data revealed comparable spectral and lifetime characteristics of NADPH produced *in vitro* from NADP-ICDH and NADPH in intracellular media-mimicking solution. In the GR catalyzed reaction, the required molar ratio GSSG/NADPH is 1. We therefore investigated whether the binding of NADPH to GR has repercussions on its spectral and lifetime properties. Blank-corrected spectra [Fig. 1(c) left] showed that the addition of GR, in the presence of GSSG, reduced (at concentration 0.5 U/ml), or nearly completely abolished (at 1 U/ml), the NADPH fluorescence produced by NADP-ICDH, while no modifications of NADPH fluorescence decays by GR were noted [Fig. 1(c) right]. This observation of the loss in the fluorescence intensity is in agreement with the dehydrogenation of NADPH to $NADP^+$ by GR [see schematic representation in Fig. 1(d)].

3.2 *HNE Decreases NAD(P)H Fluorescence in Living Cardiac Cells*

LPO, which can be initiated by free radical attack, results in the production of toxic molecules such as HNE. Oxidative stress induced by HNE was evaluated by time-resolved spectroscopy of NAD(P)H fluorescence in living cardiac myocytes [Fig. 2(a)]. HNE (25 μM) induced clear decrease in the total photon counts of NAD(P)H fluorescence [Fig. 2(b)] and this effect was more important when higher HNE concentration (50 μM) was used. We have chosen a concentration of 10 to 25 μM of HNE, which produced no toxic cell shortening [see insets of Figs. 2(b) and 3(d)] and was also used by others to test bioenergetic function in response to oxidative stress[28] to evaluate HNE-induced NAD(P)H fluorescence modifications. In addition, a concentration of 50 μM, which was described to induce protein leak through uncoupling proteins (reviewed in Ref. 29) and which provoked shortening at the cell edges in 30% of tested cells [as illustrated in the insets of Figs. 2(b) and 3(d)], was also applied to evaluate the toxic effect of lipid peroxidation on NAD(P)H content; other oxidative stress agents, such as H_2O_2, provoked similar effects on the fluorescence, as well as on the membrane quality (data not shown). These results demonstrate that HNE is

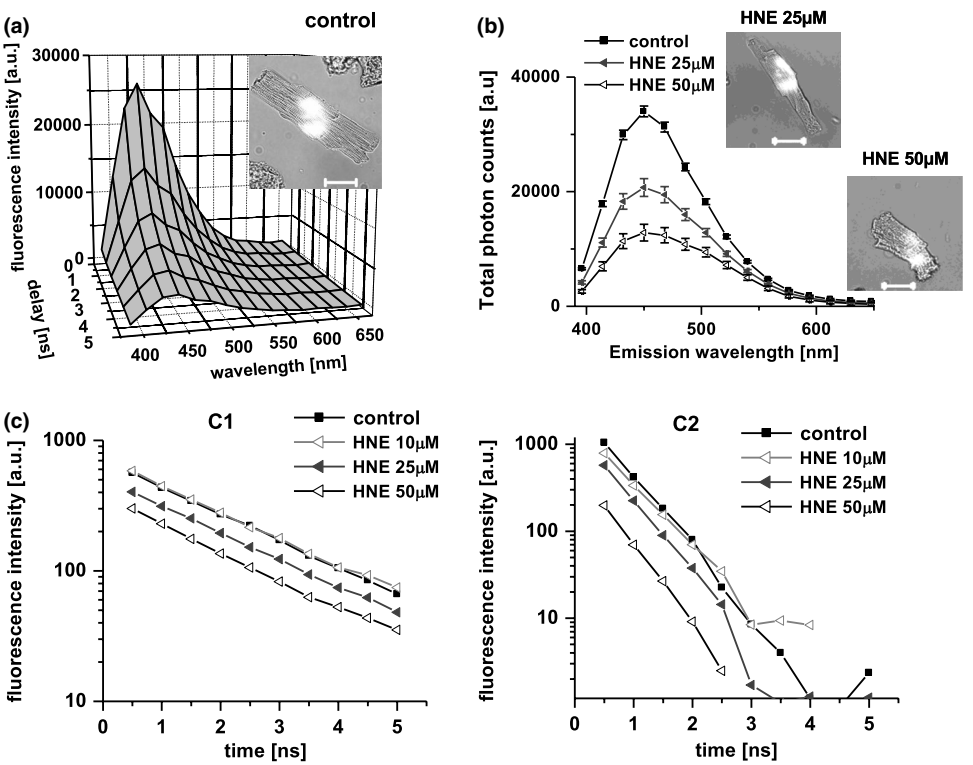

Fig. 2 NAD(P)H fluorescence in living cardiac cells and its modulation by HNE. (a) Original recording of the time-resolved spectroscopy measurements of NAD(P)H fluorescence in living cardiac cells, excitation 375 nm (mean of 10 measurements; in the inset, representative transmission image of the single cardiomyocyte illumination, scale = 33 μm). (b) Background-corrected emission spectra recorded in living cardiac cells in rising concentrations of HNE; control, $n = 78$; HNE, 25 μM, $n = 71$; HNE, 50 μM, $n = 19$; $^*p < 0.05$ versus control. (c) Individual NAD(P)H components resolved by linear unmixing of endogenous fluorescence excited at 375 nm: fluorescence decays of C1: component 1 bound NAD(P)H and C2: component 2 free NAD(P)H fluorescence is plotted in control conditions and in the presence of increasing HNE concentrations.

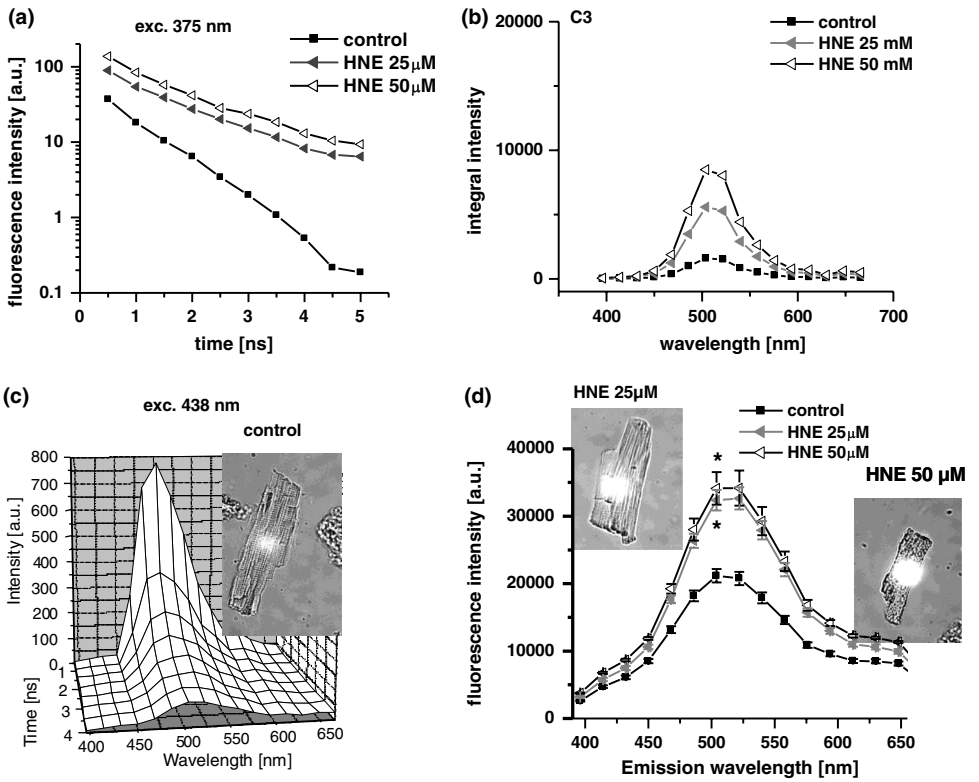

Fig. 3 Effect of HNE on flavin fluorescence in living cardiac myocytes. Effect of HNE (a) on fluorescence decays and (b) on the integral intensity spectra of the residual component, resolved by linear unmixing of endogenous fluorescence excited at 375 nm. (c) Original recording of the time-resolved spectroscopy of flavin fluorescence in living cardiac cells, excitation by 438 nm (mean of three measurements; in the inset, representative transmission image of the single cardiomyocyte illumination). (d) Effect of HNE (25 μM, $n = 21$ and 50 μM, $n = 5$) on flavin fluorescence (excited at 438 nm; in the inset, representative transmission images of the HNE-treated cardiac cells).

capable of inducing a concentration-dependent decrease in the cell NAD(P)H content.

To better understand the mechanism underlying HNE effect on the NAD(P)H content in living cardiac cells, spectral linear unmixing of NAD(P)H fluorescence components was performed. We previously reported that the recorded fluorescence has mitochondrial origins and is composed of three individual components with separate spectral characteristics:[13,14] two NAD(P)H components [Fig. 2(c)] and one residual red-shifted flavin-like component [Fig. 3(a)]. The first blue-shifted component with longer fluorescence lifetime of 2.14 ± 0.08 ns, $n = 78$ [bound NAD(P)H], had characteristics of NAD(P)H component in a more viscous environment, while the second component with faster fluorescence lifetime of 0.55 ± 0.01 ns, $n = 78$ [free NAD(P)H] had characteristics of the NAD(P)H component in a less viscous environment.

Both resolved NAD(P)H fluorescence components decreased with rising HNE concentrations [Fig. 2(c): C1 and C2] due to lower component amplitudes [Fig. 4(a) left]. At high HNE concentrations (at 50 μM), deterioration of the cell membrane could be observed in about 20% of cells [see inset of Fig. 2(b)], and at these concentrations, we also noted a change in the fluorescence lifetime of the individual components [Fig. 4(a) middle], indicating modification in the cell environment. Despite the predominant effect of HNE on the amplitude of component 2, fluorescence intensity, calculated as [(component amplitude) × (fluorescence lifetime)], revealed that component 1 is responsible for the biggest part of the lowering of the NAD(P)H fluorescence with HNE [Fig. 4(a) right]. These modifications resulted in a clear decrease of the relative spectral contribution (calculated as the fluorescence amplitude multiplied by the unitary reference spectrum reported in Ref. 13) [Fig. 4(b)], suggesting an increase in the cell oxidation. The ratio of component 2 to component 1 (free/bound) amplitude, corresponding to the change in NAD(P)H/NAD(P)$^+$ reduction/oxidation pair[18,19] and thus in the mitochondrial metabolic state, decreased with rising HNE concentrations [Fig. 4(c)]. These results were confirmed by mimicking oxidative stress conditions by the addition of H_2O_2 (1 μM) [Fig. 4(a)]. Resolved monoexponential decay for each NAD(P)H component corresponds well to the molecule in a specific state; this result is more precise than the one obtained in human myocytes,[13] possibly due to higher signal intensities in rats when compared to human.

3.3 *HNE Increases Flavoprotein Fluorescence in Living Cardiac Cells*

In addition to the two main NAD(P)H components, linear unmixing of the endogenous fluorescence also revealed presence of a small additional component. This component presented characteristics of the flavin fluorescence: emission maximum at 520 nm [Fig. 3(b)] and increase in the presence of uncouplers such as DNP (data not shown). HNE was capable of enhancing the contribution of this component in living cardiac cells [Fig. 3(b)]. To verify that this effect of HNE can indeed be attributed to flavoproteins, we have performed time-resolved spectroscopy experiments using 438-nm excitation [Fig. 3(c) and 3(d)] to favor the selective excitation of

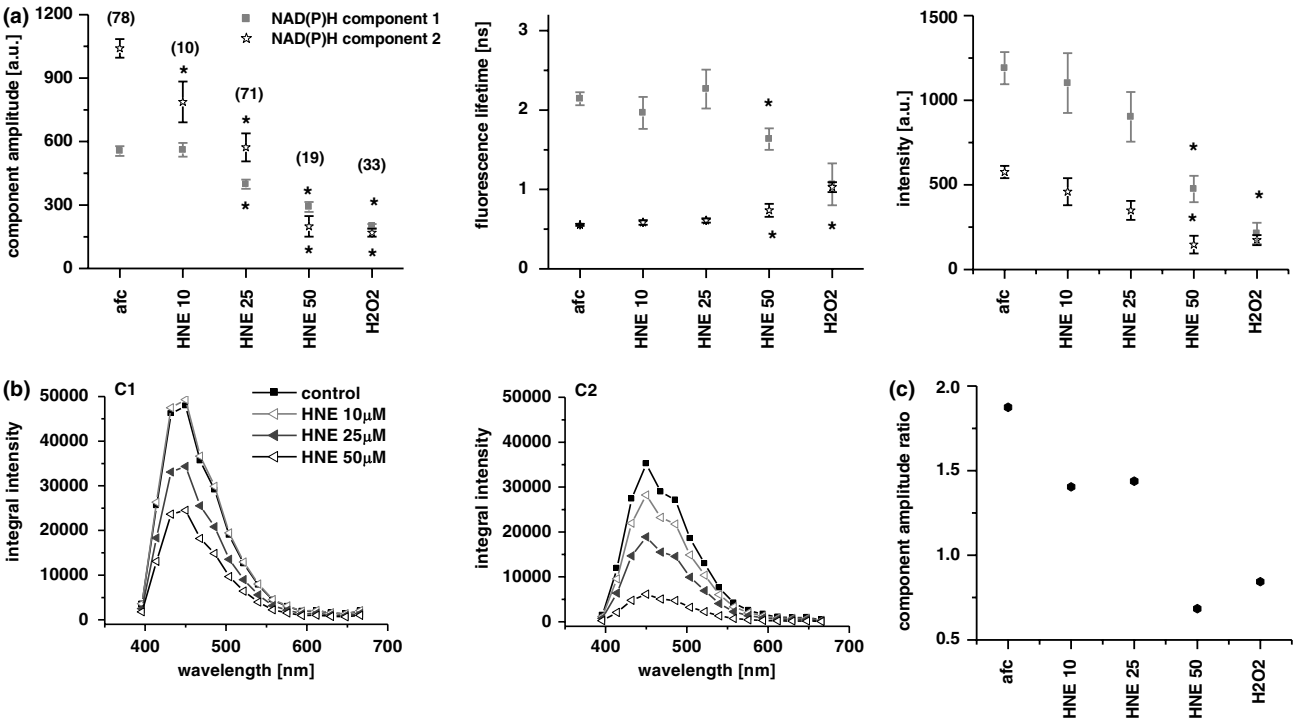

Fig. 4 Effect of HNE on individual components of NAD(P)H fluorescence. (a) The effect of HNE on the NAD(P)H fluorescence component amplitude (left), fluorescence lifetime (middle), and fluorescence intensity calculated as the component amplitude multiplied by the fluorescence lifetime of the resolved component 1 (gray squares) and component 2 (black stars) (right); the numbers represent cell number; $*p < 0.05$ versus control. (b) Integral intensity, calculated for components C1 and C2 at respective spectral channels as the component amplitude multiplied by the unitary reference spectrum. (c) Ratio of component 2 and component 1 amplitude.

flavoproteins.[30] These data clearly demonstrated a rise in the flavoprotein fluorescence by HNE (25 and 50 μM) with maximum at 500 to 520 nm, which corresponds most likely to the mixture of electron transferring flavoproteins and free FAD.[31]

GR is one of the flavoproteins that could contribute to the observed fluorescence change in cardiac cells. The activity of GR can be selectively inhibited by the chemotherapeutic drug BCNU (carmustine). The *in vitro* inhibition of GR occurred after biochemical reduction of the enzyme with NAD(P)H.[32] We have investigated the effect of HNE in the presence of the GR inhibitor BCNU (100 μM) (Fig. 5). In cells pretreated with BCNU (100 μM), we noted a decrease in the fluorescence intensity due to the reduced amplitude of component 2 [Fig. 5(a) and 5(b)]. In the presence of HNE (25 and 50 μM), BCNU induced an even further decrease of the cell autofluorescence by lowering the intensities of the two components [Fig. 5(a) and 5(b)]. We have also noted clear lowering of the component amplitude ratio and thus NAD(P)H/NAD(P)$^+$ ratio following inhibition with BCNU [Fig. 5(c)].

3.4 *HNE Increases the Percentage of Oxidized Nucleotides*

Percentage of oxidized nucleotides is an important parameter indicating cell oxidation state. To test whether HNE affects the percentage of oxidized nucleotides, cells were exposed to different concentrations of HNE and then to rotenone (1 μM) with cyanide (4 mM), or to DNP (50 μM), which were used to induce a fully reduced versus a fully oxidized state, respectively [Fig. 6(a)]. Rotenone in the presence of cyanide increased, while DNP decreased the fluorescence intensity of NAD(P)H [Fig. 6(a) and 6(c)]. Change in the percentage of oxidized nucleotides was then evaluated as fluorescence at (fully reduced—control)/(fully reduced—fully oxidized) state. Our data showed a clear rise in the percentage of oxidized nucleotides with rising concentrations of HNE [Fig. 6(b)], indicating an important cell oxidation in the presence of the LPO product. This result was verified by the addition of H_2O_2 (1 μM), a strong peroxidation agent, which was capable of inducing nearly 100% cell oxidation [Fig. 6(b)].

3.5 *HNE Lowers the Production of NADH*

HNE has been reported to reduce the production of NADH in isolated cardiac mitochondria by acting through inhibition of α-ketoglutarate dehydrogenase.[9] BHB oxidized into AcAc is known to produce NADH dependently on the BHB/AcAc ratio.[33] To investigate whether HNE is capable of affecting NADH production in living cardiac cells, we have therefore used different ratios of BHB/AcAc (20:1, condition favorable for NADH production, versus 2:1, closer to physiological condition) (Fig. 7). As expected, we observed lower fluorescence when decreasing the BHB/AcAc ratio from 20:1 to 2:1, in accordance with lower NADH concentration in cardiomyocyte mitochondria [Fig. 7(a) and 7(b)]. This effect was also observable in the presence of HNE (25 μM). Maximal production of NADH was then calculated as fluorescence at [control-(BHB:AcAc 2:1)]/[(BHB:AcAc 20:1)—(BHB:AcAc 2:1)]. In this way, we estimated maximal production of NADH to 97% in control cells before HNE application; in the presence of HNE (25 μM), it decreased to 28.6%. These experiments are in agreement with previously reported reduced NADH production by HNE.[34]

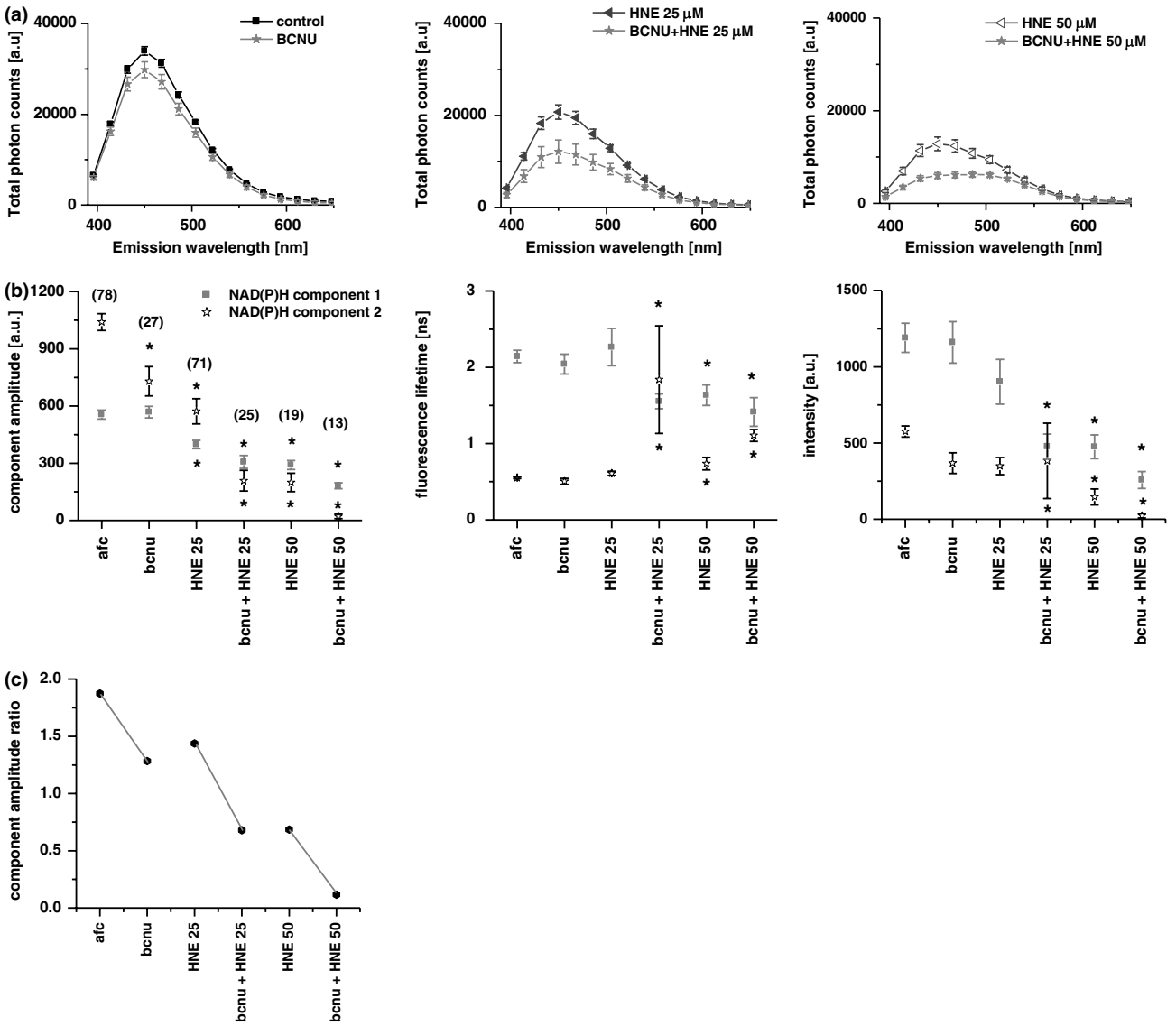

Fig. 5 Responses of NAD(P)H fluorescence to glutathione reductase inhibition in the presence and in the absence of HNE. (a) The effect of GR inhibitor BCNU (100 μM) on background-corrected emission spectra in control (left) and in the presence of HNE, 25 μM (middle) and HNE, 50 μM (right). (b) The effect of BCNU (100 μM) on the component amplitude (left), fluorescence lifetimes (middle), and the fluorescence intensity (right); the numbers represent cell number; $*p < 0.05$ versus control. (c) C2 to C1 amplitude ratio in the presence of BCNU.

4 Discussion

In this study, we investigated the effects of HNE on the regulation of endogenous NADH and NADPH mitochondrial content—for the first time in living cardiac cells—using a direct and noninvasive time-resolved fluorescence spectroscopy approach. We demonstrate that (1) HNE induced concentration-dependent decrease of NAD(P)H fluorescence due to lowering of the fluorescence from both resolved NAD(P)H components; (2) HNE increased the flavoprotein fluorescence, pointing to the contribution of flavoprotein complexes in the HNE action, and affected responsiveness of the NAD(P)H component ratio to the inhibition of GR; (3) HNE also increased the percentage of oxidized nucleotides and lowered the NADH production in cardiac cells. All together, gathered results are pointing to the fact that the lipid peroxidation product HNE provoked an important cell oxidation by acting on NAD(P)H regulating systems in the heart.

Aerobic organisms are dependent upon the varying intracellular concentrations of NADH and NADPH. The former is the primary ingredient that fuels adenosine trisphosphate (ATP) production in mitochondria via oxidative phosphorylation, while the latter helps to sustain the reductive environment necessary for this process and other cellular activities. Beyond the role of mitochondria in ATP production, these organelles are also implicated in most diseases, mainly due to their involvement in the energy production and cellular functioning. Previous observations[35] showed a correlation between the rise in generation of reactive oxygen species (ROS), increase in cellular contractility, and decrease in the NAD(P)H fluorescence under physiological conditions. However, studies performed directly in living cardiac cells, in order to better understand the involved mechanisms, are still missing. We have previously reported that oxidative stress induced by HNE or H_2O_2 decreases endogenous mitochondrial NAD(P)H fluorescence of LV myocytes

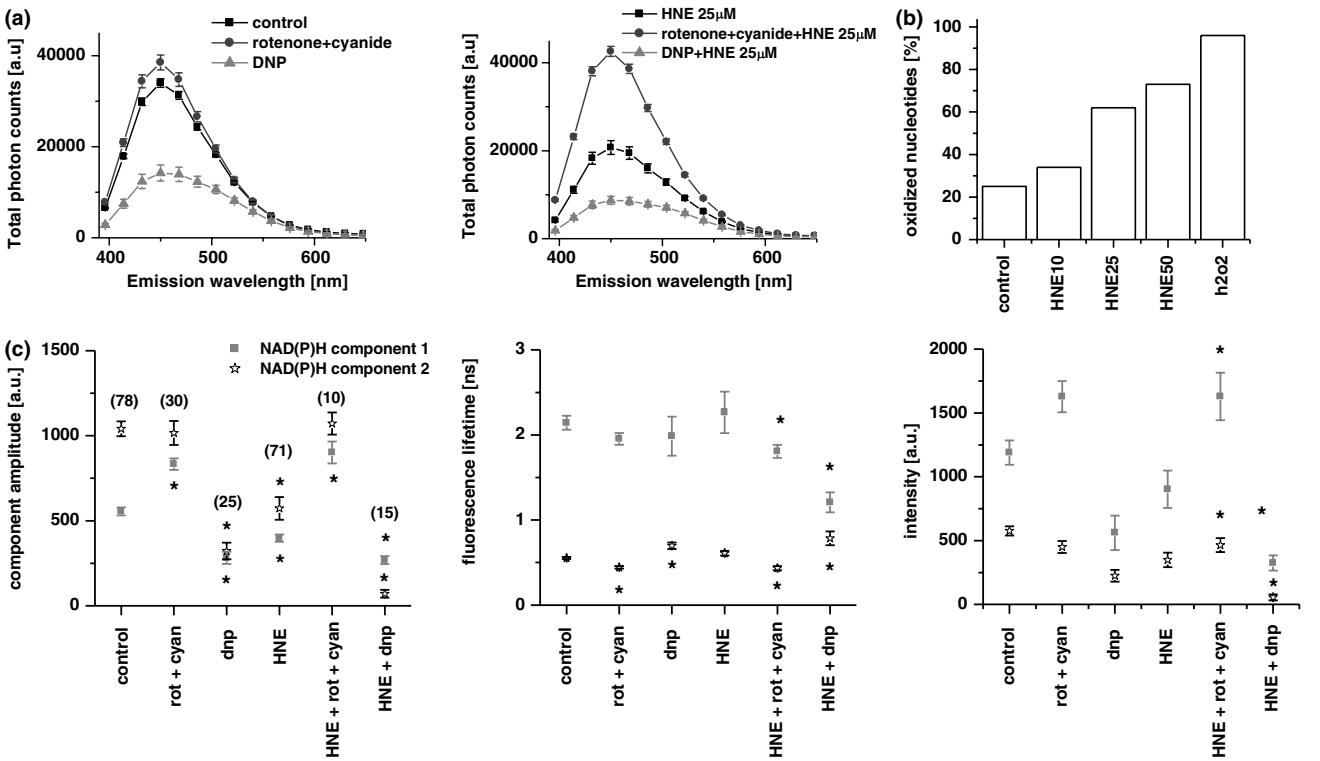

Fig. 6 Effect of HNE on the percentage of oxidized nucleotides in cardiac cells. (a) Background-corrected emission spectra of the NAD(P)H fluorescence in control conditions, $n = 78$ and in fully reduced state after treatment with rotenone with cyanide (1 μM and 4 mM, respectively, $n = 30$), or in fully oxidized state after treatment with DNP (50 μM, $n = 15$) (left) and cells treated with HNE (25 μM, $n = 74$) and after treatment with rotenone with cyanide (1 μM and 4 mM respectively, $n = 25$), or with DNP (50 μM, $n = 15$) (right). (b) Percentage of oxidized nucleotides, calculated as fluorescence at (fully reduced – control) / (fully reduced – fully oxidized) state in different HNE concentrations and/or in the presence of H_2O_2. (c) Component amplitude (left), fluorescence lifetimes (middle), and fluorescence intensity (right) of C1 and C2 in the presence of rotenone with cyanide (1 μM and 4 mM, respectively), or DNP (50 μM); the cell number is in brackets; $^*p < 0.05$ versus Control.

(see Supplement in Ref. 10) and demonstrated that the contractility is inversely correlated with NAD(P)H content.[10] Here, we evaluated in further detail the effects underlying HNE actions.

The role of mitochondrial NADP-ICDH in controlling the mitochondrial redox balance and subsequent cellular defense against oxidative injury was demonstrated as a major NADPH producer in the mitochondria.[25,26] Although some $NADP^+$ can be converted into $NADP^+$ by NAD^+ kinase (NADKase), which phosphorylates NAD^+ (Refs. 36 and 37), the major source of NADPH in most cells is the oxidative phase of the pentose phosphate pathway (PPP). However, in the heart, the capacity of oxidative PPP is low[38] due to the limited activity of glucose-6-phosphate dehydrogenase (G-6-PDH).[39] NADPH can also be produced by the activity of the malic enzyme and of the NADP-ICDH in the cytosol as well as the mitochondria, using $NADP^+$ as a cofactor instead of NAD^+. The $NADPH/NADP^+$ ratio can also be modulated by the activity of the H^+-transhydrogenases driven by the proton electrochemical gradient.[40,41]

HNE, one of the major secondary byproducts of LPO, inactivates the rate-limiting enzymes of the glycolytic pathway and the PPP.[42] Under normal conditions, G-6-PDH is inhibited by NADPH. This can be overcome by increasing the oxidized glutathione and by elevating the $NADP^+/NADPH$ ratio. Stimulation of this pathway can be one side-effect of HNE; fundamental function of PPP is to maintain GSH in a reduced state in order to protect cellular integrity from emerging oxygen radicals.[43] Previous studies[6] demonstrated that HNE is capable of decreasing the NADP-ICDH activity in mitochondria via enzyme inactivation, based on the measurement of the enzyme protein expression. Such actions explain the decrease in the amount of NADPH recorded in the present study.

Production of NADPH required for the regeneration of glutathione in the mitochondria is critical for scavenging mitochondrial ROS through GR and peroxidase systems. Our data gathered *in vitro* demonstrated that NADPH fluorescence intensity is sensitive to dehydrogenation by GR. Our measurements of the flavoprotein fluorescence confirmed that the action of HNE affects the flavoproteins. Consequently, the decrease in the first bound NAD(P)H component with HNE is related to the stimulation of flavoproteins. This effect contributed to decrease in the free/bound component ratio and thus to the regulation of the $NAD(P)H/NAD(P)^+$ ratio in cardiac cells by HNE.

NADPH dehydrogenation by GR was tested in single cells using BCNU, an agent that is widely used in the chemotherapy of brain tumors, which has been shown to inhibit GR, the enzyme that catalyzes the recycling of GSH from oxidized GSSG.[44] The inhibition of GR results in the depletion of GSH and the accumulation of GSSG,[45,46] which is likely to compromise cellular oxidative defenses that rely on antioxidant actions of reduced glutathione.[47] Indeed, BCNU-treated cells have been reported to be more vulnerable to oxidative stress.[46] Decreased levels of cellular GSH have been linked to the increased production of ROS, dysregulation, opening of the mitochondrial permeability transition pore, and cell death.[48–52] At concentrations from 50 μg/ml, the GR-inhibitor BCNU also

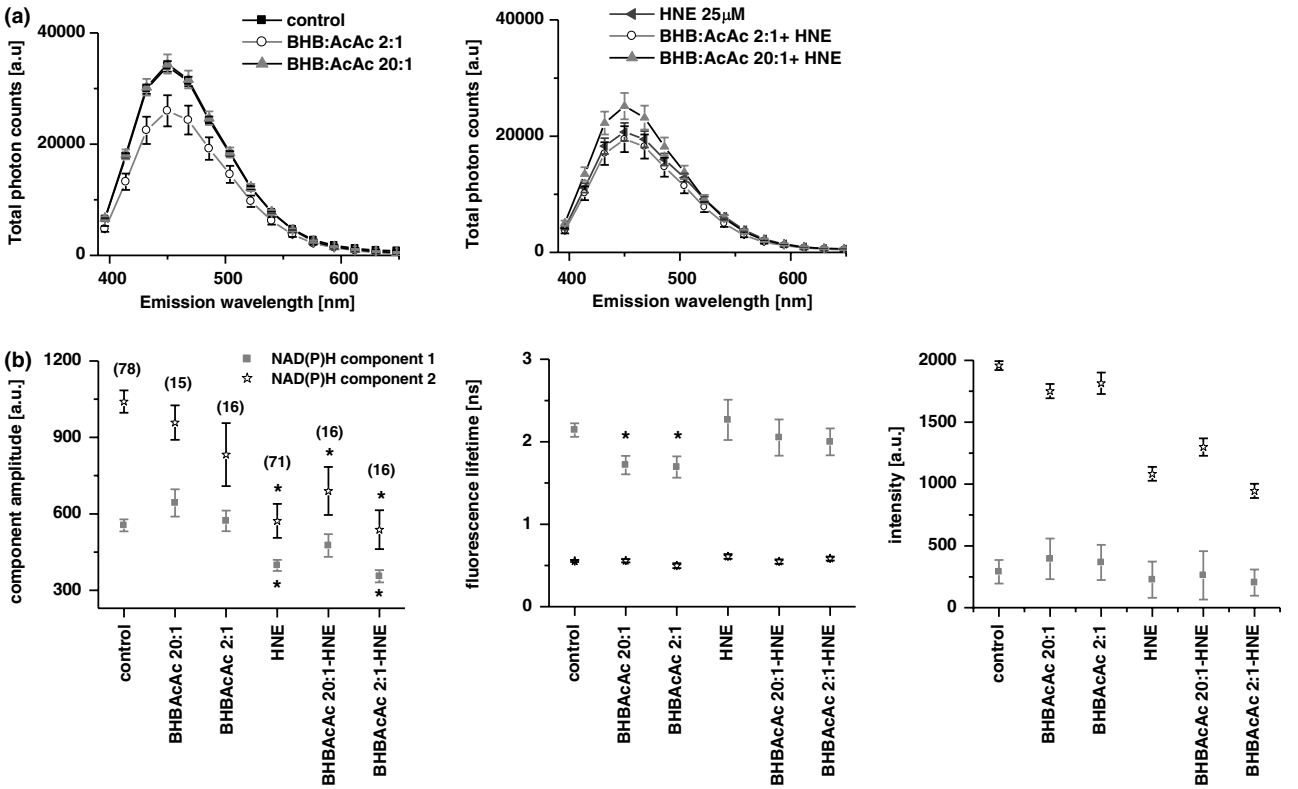

Fig. 7 Effect of HNE on the NADH production in cardiac cells. (a) Background-corrected emission spectra of the NAD(P)H fluorescence in control conditions ($n = 78$) and/or treated with BHB/AcAc 20:1 ($n = 35$), or BHB/AcAc 2:1 ($n = 18$) (left) and in cells treated with HNE (25 μM, $n = 71$) alone and/or treated with BHB/AcAc 20:1 ($n = 16$), or BHB/AcAc 2:1 ($n = 16$) (right). (b) Component amplitude (left), fluorescence lifetimes (middle), and fluorescence intensity (right) of C1 and C2 in the presence of different BHB/AcAc ratio; the cell number is in brackets; $^*p < 0.05$ versus control.

decreased flux through the PPP.[53] Beyond the complex effects of BCNU on the generation of ROS and apoptosis,[32] the inhibitor of GR induced decrease in both components, with a more important effect at the free NAD(P)H. This result points to GR as one of the potential flavoproteins affected by HNE.

NADH, which is generated essentially during the catabolism of acetyl-coenzyme A via the tricarboxylic acid cycle, is considered a powerful pro-oxidant as its downstream metabolism is mediated by complexes I, III, and IV, and produces most probably the majority of ROS generated in aerobic organisms.[54] Hence, a fine balance has to be maintained between these two nicotinamide nucleotides for an optimal cell functioning with adequate levels of NADPH and ATP and a small amount of NADH. In isolated cardiac mitochondria, it has been reported that HNE inhibited α-ketoglutarate dehydrogenase and reduced the production of NADH.[9] Our data demonstrated that HNE also decreased the NADH production in living cardiac cells. In addition, we have observed a concentration-dependent increase in the percentage of oxidized nucleotides with HNE as well. All these observations point toward an important cell oxidation induced by HNE by acting on NAD(P)H regulating systems in living cardiac cells. This process is part of the complex inhibitory effect of this compound on cell respiration and concomitant with protein modification and cell death.[55]

5 Conclusions

Our results shed a new light on the effect of HNE on the regulation of NAD(P)H in living cardiac cells. We propose that HNE reduces NAD(P)H content via a decrease in the production of NADH, stimulation of NAD(P)H use by flavoprotein complexes and, consequently, provokes an important cell oxidation by dehydrogenation of both free and bound NAD(P)H molecules in living cells. This action is likely to affect the overall energy production and use in the heart. However, future studies are necessary to explain precisely the mechanisms responsible for HNE-induced changes. It is now well established that mitochondria is an important target for oxidative stress in a broad range of pathologies, including cardiovascular disease, diabetes, neurodegeneration, and cancer. Understanding the precise role of oxidative processes and their products in living cells is crucial for finding new noninvasive tools for biomedical diagnostics of pathophysiological conditions.

Acknowledgments

The authors acknowledge support from Integrated Initiative of European Laser Infrastructures LASERLAB-EUROPE III (grant agreement no. 284464, EC's Seventh Framework Programme) and the Research grant agency of the Ministry of Education, Science, Research and Sport of the Slovak Republic VEGA No 1/0296/11, VEGA No 2/0094/12, and APVV-0242-11. This study was also supported by grants to A.C. from the Canadian Institutes Health Research (MOP 84450), and the Heart and Stroke Foundation of Quebec. S.A. was a recipient of the studentship from Libyan Ministry of Superior Studies. We would like to thank C. Des Rosiers for the generous gift of AcAc.

References

1. H. Esterbauer, R. J. Schaur, and H. Zollner, "Chemistry and biochemistry of 4-hydroxynonenal, malonaldehyde and related aldehydes," *Free Radic. Biol. Med.* **11**(1), 81–128 (1991).
2. C. X. Santos et al., "Redox signaling in cardiac myocytes," *Free Radic. Biol. Med.* **50**(7), 777–793 (2011).
3. C. Schneider, N. A. Porter, and A. R. Brash, "Routes to 4-hydroxynonenal: fundamental issues in the mechanisms of lipid peroxidation," *J. Biol. Chem.* **283**(23), 15539–15543 (2008).
4. Y. C. Awasthi et al., "Regulation of 4-hydroxynonenal-mediated signaling by glutathione S-transferases," *Free Radic. Biol. Med.* **37**(5), 607–619 (2004).
5. S. Dwivedi et al., "Role of 4-hydroxynonenal and its metabolites in signaling," *Redox. Rep.* **12**(1), 4–10 (2007).
6. M. Benderdour et al., "Cardiac mitochondrial NADP+-isocitrate dehydrogenase is inactivated through 4-hydroxynonenal adduct formation: an event that precedes hypertrophy development," *J. Biol. Chem.* **278**(46), 45154–45159 (2003).
7. M. Benderdour et al., "Decreased cardiac mitochondrial NADP+-isocitrate dehydrogenase activity and expression: a marker of oxidative stress in hypertrophy development," *Am. J. Physiol. Heart Circ. Physiol.* **287**(5), H2122–H2131 (2004).
8. J. H. Yang, E. S. Yang, and J. W. Park, "Inactivation of $NADP^+$-dependent isocitrate dehydrogenase by lipid peroxidation products," *Free Radic. Res.* **38**(3), 241–249 (2004).
9. K. M. Humphries and L. I. Szweda, "Selective inactivation of alpha-ketoglutarate dehydrogenase and pyruvate dehydrogenase: reaction of lipoic acid with 4-hydroxy-2-nonenal," *Biochemistry* **37**(45), 15835–15841 (1998).
10. V. Bassien-Capsa et al., "Metabolic remodelling of cardiac myocytes during pregnancy: the role of mineralocorticoids," *Can. J. Cardiol.* **27**(6), 834–842 (2011).
11. D. Chorvat, Jr. and A. Chorvatova, "Multi-wavelength fluorescence lifetime spectroscopy: a new approach to the study of endogenous fluorescence in living cells and tissues," *Laser Phys. Lett.* **6**(3), 175–193 (2009).
12. S. Aneba et al., "Probing of cardiomyocyte metabolism by spectrally resolved lifetime detection of NAD(P)H fluorescence," *Comput. Cardiol.* **34**, 349–352 (2007).
13. D. Chorvat, Jr. et al., "Rejection of transplanted hearts in patients evaluated by the component analysis of multi-wavelength NAD(P)H fluorescence lifetime spectroscopy," *J. Biophoton.* **3**(10–11), 646–652 (2010).
14. A. Chorvatova et al., "Effect of ouabain on metabolic oxidative state in living cardiomyocytes evaluated by time-resolved spectroscopy of endogenous NAD(P)H fluorescence," *J. Biomed. Opt.* **17**(10), 101505 (2012).
15. P. D. Reiss, P. F. Zuurendonk, and R. L. Veech, "Measurement of tissue purine, pyrimidine, and other nucleotides by radial compression high-performance liquid chromatography," *Anal. Biochem.* **140**(1), 162–171 (1984).
16. R. L. Veech, "The metabolism of lactate," *NMR Biomed.* **4**(2), 53–58 (1991).
17. S. J. Lin and L. Guarente, "Nicotinamide adenine dinucleotide, a metabolic regulator of transcription, longevity and disease," *Curr. Opin. Cell Biol.* **15**(2), 241–246 (2003).
18. D. K. Bird et al., "Metabolic mapping of MCF10A human breast cells via multiphoton fluorescence lifetime imaging of the coenzyme NADH," *Cancer Res.* **65**(19), 8766–8773 (2005).
19. R. Niesner et al., "Noniterative biexponential fluorescence lifetime imaging in the investigation of cellular metabolism by means of NAD(P)H autofluorescence," *Chemphyschem.* **5**(8), 1141–1149 (2004).
20. V. Bassien-Capsa, E. De Smet, and A. Chorvatova, "Structure/function modifications of single left ventricular cardiomyocytes in pregnancy and experimental preeclampsia in rats," *Circulation* **111**(4), E76–E77 (2005).
21. V. Bassien-Capsa et al., "Structural, functional and metabolic remodeling of rat left ventricular myocytes in normal and in sodium-supplemented pregnancy," *Cardiovasc. Res.* **69**(2), 423–431 (2006).
22. D. Chorvat, Jr. and A. Chorvatova, "Spectrally resolved time-correlated single photon counting: a novel approach for characterization of endogenous fluorescence in isolated cardiac myocytes," *Eur. Biophys. J. Biophys. Lett.* **36**(1), 73–83 (2006).
23. M. Wakita, G. Nishimura, and M. Tamura, "Some characteristics of the fluorescence lifetime of reduced pyridine nucleotides in isolated mitochondria, isolated hepatocytes, and perfused rat liver in situ," *J. Biochem. (Tokyo)* **118**(6), 1151–1160 (1995).
24. A. Gafni and L. Brand, "Fluorescence decay studies of reduced nicotinamide adenine dinucleotide in solution and bound to liver alcohol dehydrogenase," *Biochemistry* **15**(15), 3165–3171 (1976).
25. S. H. Jo et al., "Control of mitochondrial redox balance and cellular defense against oxidative damage by mitochondrial NADP+-dependent isocitrate dehydrogenase," *J. Biol. Chem.* **276**(19), 16168–16176 (2001).
26. H. J. Koh et al., "Cytosolic $NADP^+$-dependent isocitrate dehydrogenase plays a key role in lipid metabolism," *J. Biol. Chem.* **279**(38), 39968–39974 (2004).
27. S. Curello et al., "Changes in the cardiac glutathione status after ischemia and reperfusion," *Experientia* **41**(1), 42–43 (1985).
28. B. P. Dranka et al., "Assessing bioenergetic function in response to oxidative stress by metabolic profiling," *Free Radic. Biol. Med.* **51**(9), 1621–1635 (2011).
29. R. J. Mailloux and M. E. Harper, "Uncoupling proteins and the control of mitochondrial reactive oxygen species production," *Free Radic. Biol. Med.* **51**(6), 1106–1115 (2011).
30. B. Chance et al., "Oxidation-reduction ratio studies of mitochondria in freeze-trapped samples. NADH and flavoprotein fluorescence signals," *J. Biol. Chem.* **254**(11), 4764–4771 (1979).
31. D. Chorvat, Jr. et al., "Spectral unmixing of flavin autofluorescence components in cardiac myocytes," *Biophys. J.* **89**(6), L55–L57 (2005).
32. J. M. An et al., "Carmustine induces ERK- and JNK-dependent cell death of neuronally-differentiated PC12 cells via generation of reactive oxygen species," *Toxicol. In Vitro* **25**(7), 1359–1365 (2011).
33. L. H. Opie and P. Owen, "Effects of increased mechanical work by isolated perfused rat heart during production or uptake of ketone bodies. Assessment of mitochondrial oxidized to reduced free nicotinamide-adenine dinucleotide ratios and oxaloacetate concentrations," *Biochem. J.* **148**(3), 403–415 (1975).
34. K. M. Humphries, Y. Yoo, and L. I. Szweda, "Inhibition of NADH-linked mitochondrial respiration by 4-hydroxy-2-nonenal," *Biochemistry* **37**(2), 552–557 (1998).
35. F. R. Heinzel et al., "Formation of reactive oxygen species at increased contraction frequency in rat cardiomyocytes," *Cardiovasc. Res.* **71**(2), 374–382 (2006).
36. G. Magni, G. Orsomando, and N. Raffaelli, "Structural and functional properties of NAD kinase, a key enzyme in NADP biosynthesis," *Mini. Rev. Med. Chem.* **6**(7), 739–746 (2006).
37. R. Singh et al., "Oxidative stress evokes a metabolic adaptation that favors increased NADPH synthesis and decreased NADH production in pseudomonas fluorescens," *J. Bacteriol.* **189**(18), 6665–6675 (2007).
38. R. L. Jolley, V. H. Cheldelin, and R. W. Newburgh, "Glucose catabolism in fetal and adult heart," *J. Biol. Chem.* **233**(6), 1289–1294 (1958).
39. H. G. Zimmer, "The oxidative pentose phosphate pathway in the heart: regulation, physiological significance, and clinical implications," *Basic Res. Cardiol.* **87**(4), 303–316 (1992).
40. L. A. Sazanov and J. B. Jackson, "Proton-translocating transhydrogenase and NAD- and NADP-linked isocitrate dehydrogenases operate in a substrate cycle which contributes to fine regulation of the tricarboxylic acid cycle activity in mitochondria," *FEBS Lett.* **344**(2–3), 109–116 (1994).
41. B. Comte et al., "Reverse flux through cardiac NADP(+)-isocitrate dehydrogenase under normoxia and ischemia," *Am. J. Physiol. Heart Circ. Physiol.* **283**(4), H1505–H1514 (2002).
42. I. Miwa et al., "4-Hydroxy-2-nonenal hardly affects glycolysis," *Free Radic. Biol. Med.* **23**(4), 610–615 (1997).
43. F. Puskas et al., "Stimulation of the pentose phosphate pathway and glutathione levels by dehydroascorbate, the oxidized form of vitamin C," *FASEB J.* **14**(10), 1352–1361 (2000).
44. H. Frischer and T. Ahmad, "Severe generalized glutathione reductase deficiency after antitumor chemotherapy with BCNU" [1,3-bis(chloroethyl)-1-nitrosourea]," *J. Lab Clin. Med.* **89**(5), 1080–1091 (1977).
45. A. C. Smith and M. R. Boyd, "Preferential effects of 1,3-bis(2-chloroethyl)-1-nitrosourea (BCNU) on pulmonary glutathione reductase and glutathione/glutathione disulfide ratios: possible implications for lung toxicity," *J. Pharmacol. Exp. Ther.* **229**(3), 658–663 (1984).

46. W. Ma et al., "Peroxide toxicity in conditioned lens epithelial cells—Evaluation of multi-defense systems," *Exp. Eye Res.* **77**(6), 711–720 (2003).
47. A. Meister, "Glutathione-ascorbic acid antioxidant system in animals," *J. Biol. Chem.* **269**(13), 9397–9400 (1994).
48. C. M. Pereira and C. R. Oliveira, "Glutamate toxicity on a PC12 cell line involves glutathione (GSH) depletion and oxidative stress," *Free Radic. Biol. Med.* **23**(4), 637–647 (1997).
49. O. P. Jurma, D. G. Hom, and J. K. Andersen, "Decreased glutathione results in calcium-mediated cell death in PC12," *Free Radic. Biol. Med.* **23**(7), 1055–1066 (1997).
50. P. Froissard, H. Monrocq, and D. Duval, "Role of glutathione metabolism in the glutamate-induced programmed cell death of neuronal-like PC12 cells," *Eur. J. Pharmacol.* **326**(1), 93–99 (1997).
51. O. A. Bizzozero et al., "Acute depletion of reduced glutathione causes extensive carbonylation of rat brain proteins," *J. Neurosci. Res.* **83**(4), 656–667 (2006).
52. D. Shen et al., "Glutathione redox state regulates mitochondrial reactive oxygen production," *J. Biol. Chem.* **280**(27), 25305–25312 (2005).
53. A. C. Williams and W. C. Ford, "Functional significance of the pentose phosphate pathway and glutathione reductase in the antioxidant defenses of human sperm," *Biol. Reprod.* **71**(4), 1309–1316 (2004).
54. P. Jezek and L. Hlavata, "Mitochondria in homeostasis of reactive oxygen species in cell, tissues, and organism," *Int. J. Biochem. Cell Biol.* **37**(12), 2478–2503 (2005).
55. B. G. Hill et al., "Importance of the bioenergetic reserve capacity in response to cardiomyocyte stress induced by 4-hydroxynonenal," *Biochem. J.* **424**(1), 99–107 (2009).